been described (*21*). Kinase assays were performed on immunoprecipitated material from 100-ml cultures for 20 min at 30°C as described (*37*). Kinase reactions also contained 100 ng of purified PHO4 (*16*), 1 μg of histone HI (Boehringer Mannheim), 1 μg of β-casein (Sigma), or 1 μg of myelin basic protein (Sigma) as indicated. The background kinase activity associates nonspecifically with protein A–Sepharose beads (*16*).

29. S. Reed, J. Hadwiger, A. Lorincz, *Proc. Natl. Acad. Sci. U.S.A.* **82**, 4055 (1985).
30. Strain K699a [**a** *ade2-1 trp1-1 leu2-3,112 his3-11 ura3 can1-100* (*5*)] was grown in YEPD to 5 × 10^6 cells per milliliter at 25°C. Cells were arrested for 160 min at 25°C with 5 μM α factor (Vetrogen, London, Ontario). Cells were centrifuged, washed with cold YEPD, and reinoculated into fresh YEPD. A sample was taken at this point and every following 20 min and analyzed for RNA, kinase activity, DNA content, and budding as previously described (*37*). Cells were prepared for fluorescence-activated cell sorting (FACS) analysis on a Becton Dickinson FACSCAN as described (*5*), and results were analyzed with LYSYS II software (Becton Dickinson). Total RNA was isolated from 10 ml of cells, and 7.5 μg was transferred to nylon membrane and probed as described (*37*). The probes used were a fragment containing the *PCL2* gene from pAS-*PCL2* (*20*), a fragment corresponding to the exact *CLN2* open reading frame (*38*), and a 600-bp Eco RI to Hind III fragment of the *ACT1* gene.
31. For protein immunoblotting of PHO85, 40 μg of lysate was diluted into SDS–polyacrylamide gel electrophoresis (SDS-PAGE) sample buffer, boiled, and loaded onto a 10% gel. A chemiluminescence system was used for immunoblot detection (DuPont). PHO85 antiserum was diluted 1:1000; secondary antibodies conjugated to horseradish peroxidase (Bio-Rad) were diluted 1:10,000.
32. The strains used to construct the quadruple mutant were BY376, **a** *cln1ΔTRP1 cln2ΔLEU2 pcl2ΔLYS2 his3Δ200 lys2-801ᵃ ade2-107°*; and BY377, α *cln1ΔTRP1 pcl2ΔLYS2 hcs26ΔHIS3 leu2-Δ1 lys2-801ᵃ ade2-107°*. These strains are isogenic to strain BY263 (*28*). Construction of the *cln1ΔTRP1* and *hcs26ΔHIS3* alleles [(*14*); J. Ogas, thesis, University of California, San Francisco, CA (1992)] and the *cln2ΔLEU2* allele has been described (*38*). The *pcl2ΔLYS2* allele was constructed by PCR as described (*28*). To rescue the quadruple mutant, we transformed plasmid p*GAL-CLN1-URA3-LEU2* [YCpG3 (*38*)] into strains BY376 and BY377. The transformants were mated, and the quadruple knockout was recovered by dissecting tetrads on galactose medium. BY472A and BY472B are two independent quadruple mutants rescued from this cross. To examine the arrest phenotype, we grew cultures to a density of approximately 1 × 10^7 cells per milliliter in synthetic galactose (SG) medium. A logarithmic phase sample was removed, and 2% glucose was added to the culture to repress expression of *GAL-CLN1*. Samples were taken at the indicated time points (Fig. 4), fixed, and stained as described (*30*) for FACS analysis. Cells were photographed with Kodak Technical Pan film with a Nikon Microphot FXA microscope equipped with Nomarski optics.
33. B. Andrews and V. Measday, unpublished data.
34. The strains used to construct the triple *pho85Δ cln1Δ cln2Δ* mutant were BY442, **a** *cln2ΔURA3 pho85ΔLEU2 trp1Δ63 lys2-801ᵃ ade2-107° his3Δ200*; and BY438, α *cln1ΔTRP1 cln2ΔURA3 lys2-801ᵃ ade2-107° his3Δ200 leu2-Δ1*. The *cln2ΔURA3* allele is a complete open reading frame deletion of *CLN2* (M. Tyers, unpublished data). The strains were transformed with plasmid p*GAL-PHO85-HIS3*, and the triple mutant was rescued as described (*32*). The *GAL-PHO85* plasmid was constructed by insertion of a fragment carrying the *PHO85* cDNA from plasmid pSY854 into a *GAL* promoter derivative of pRS313 [R. Sikorski and P. Hieter, *Genetics* **122**, 19 (1989)].
35. V. Measday, unpublished data.
36. Y. Ueda, A. Toh-e, Y. Oshima, *J. Bacteriol.* **122**, 911 (1975).
37. M. Tyers, G. Tokiwa, R. Nash, B. Futcher, *EMBO J.* **11**, 1173 (1992).
38. J. Hadwiger *et al.*, *Proc. Natl. Acad. Sci. U.S.A.* **86**, 6255 (1989).
39. I. Wilson *et al.*, *Cell* **37**, 767 (1984).
40. We thank H. Espinoza, D. Morgan, and E. O'Shea for discussing unpublished results; E. O'Shea for providing PHO4; B. Dietrich for the pE719-HMK vector; A. Spence for help with microscopy and photography; C. Smith for help with FACS; A. Toh-e for *PHO85* plasmids; S. Elledge for the yeast cDNA library; A. Nieman for helpful discussions; and L. Harrington, A. Spence, and M. Donoviel for comments on the manuscript. V.M. holds a University of Toronto Open Fellowship. J.O. was supported by a fellowship from the Ford Foundation. Supported by grants from the National Cancer Institute (NCI) of Canada with funds from the Canadian Cancer Society and the Terry Fox Run to B.J.A. and M.T. B.J.A. is a scholar of the Medical Research Council of Canada and M.T. is a NCI of Canada Research Scientist.

15 July 1994; accepted 30 September 1994

Lymphotactin: A Cytokine That Represents a New Class of Chemokine

Gregory S. Kelner, Jacqueline Kennedy, Kevin B. Bacon, Sarah Kleyensteuber, David A. Largaespada, Nancy A. Jenkins, Neal G. Copeland, J. Fernando Bazan, Kevin W. Moore, Thomas J. Schall, Albert Zlotnik*

In this study, the cytokine-producing profile of progenitor T cells (pro-T cells) was determined. During screening of a complementary DNA library generated from activated mouse pro-T cells, a cytokine designated lymphotactin was discovered. Lymphotactin is similar to members of both the Cys-Cys and Cys-X-Cys chemokine families but lacks two of the four cysteine residues that are characteristic of the chemokines. Lymphotactin is also expressed in activated $CD8^+$ T cells and $CD4^-CD8^-$ T cell receptor $\alpha\beta^+$ thymocytes. It has chemotactic activity for lymphocytes but not for monocytes or neutrophils. The gene encoding lymphotactin maps to chromosome one. Taken together, these observations suggest that lymphotactin represents a novel addition to the chemokine superfamily.

The pro-T cell is an immature thymocyte subset that is likely to be the final differentiation stage before the onset of T cell receptor (TCR) β chain gene rearrangement (*1*, *2*). These cells are phenotypically characterized by the surface expression of both CD25 and CD44 and by lack of surface expression of CD3, CD4, and CD8. Pro-T cells can produce high titers of interleukin-2 (IL-2), tumor necrosis factor α (TNF-α), and interferon γ (IFN-γ) when activated in vitro with phorbol 12-myristate 13-acetate (PMA), calcium ionophore A23187, and IL-1 (*3*). We screened a complementary DNA (cDNA) library generated from activated pro-T cells in an attempt to identify new cytokines. Here we describe such a cytokine, which has chemotactic activities that appear to be specific for lymphocytes.

To characterize the cytokine-producing potential of pro-T cells, both in vitro activated and freshly sorted pro-T cells were analyzed by polymerase chain reaction (PCR). Pro-T cells activated in vitro with PMA, A23187, and IL-1 produced mRNA for IL-2, IFN-γ, TNF-α, granulocyte-macrophage colony-stimulating factor (GM-CSF), and both the p35 and p40 chains of IL-12. No mRNA for IL-4 or IL-10 was detected. Similarly, freshly sorted pro-T cells were shown to contain mRNA for IL-2, IFN-γ, TNF-α, and GM-CSF. Again, no message for IL-4 or IL-10 was detected, and there was no message for either the p35 or p40 chain of IL-12. This common mRNA cytokine profile of freshly sorted pro-T cells and pro-T cells activated in vitro suggests that the pro-T cells are activated in vivo. To further verify the cytokine-producing potential of pro-T cells, a Southern (DNA) blot of an activated pro-T cell cDNA library was probed. IL-2, IL-3, GM-CSF, IFN-γ, and the p40 chain of IL-12 were detected in this library.

During screening of the pro-T cell cDNA library, a clone was isolated (Fig. 1A), the protein translation of which consistently matched a short COOH-terminal segment of Cys-Cys chemokine protein chains in BLAST searches of protein and nucleic acid databases (*4*). A weaker similarity in this region was also noted with Cys-X-Cys chemokine sequences. Because of its biological activities described below,

G. S. Kelner, J. Kennedy, K. B. Bacon, S. Kleyensteuber, J. F. Bazan, K. W. Moore, T. J. Schall, A. Zlotnik, Department of Immunology, DNAX Research Institute of Cellular and Molecular Biology, Palo Alto, CA 94304, USA.
D. A. Largaespada, N. A. Jenkins, N. G. Copeland, Mammalian Genetics Laboratory, Advanced Biosciences Laboratories Basic Research Program, National Cancer Institute–Frederick Cancer Research and Development Center, Frederick, MD 21702, USA.

*To whom correspondence should be addressed at DNAX Research Institute of Cellular and Molecular Biology, 901 California Avenue, Palo Alto, CA 94304, USA.

we designated this molecule lymphotactin.

A closer comparison of lymphotactin with members of both the Cys-Cys and Cys-X-Cys chemokine families has yielded insight into its possible origin. In Fig. 1B, the amino acid sequences of macrophage inflammatory protein 1β (MIP-1β) and Gro-α, respectively representative of Cys-Cys and Cys-X-Cys chemokines (*5*), are shown, based on the conserved exon organization of their chemokine gene families. Alignment of the lymphotactin sequence with these molecules shows that the highest degree of identity occurs within exon three equivalents. The Cys-Cys and Cys-X-Cys chemokine families are defined by two structurally conserved cysteine residues in their respective protein NH_2-termini, which in turn form part of two distinct disulfide links to a pair of cysteine residues located at the COOH-terminal. The lymphotactin sequence lacks the first cysteine residue of the distinctive NH_2-terminal Cys-Cys or Cys-X-Cys motifs, as well as the corresponding disulfide partner elsewhere in the chain (Fig. 1B). Therefore, lymphotactin maintains only one of the two disulfide bridges (Cys^2-Cys^4) of the chemokine fold (*6*). Aside from this, lymphotactin appears to be more closely related to the Cys-Cys chemokine family, as judged by sparse sequence patterns that are diagnostic of Cys-Cys chemokines (*7*). Specifically, a phenylalanine and a tyrosine residue (Fig. 1B) that are characteristic of the Cys-Cys chemokine family but not found in the Cys-X-Cys family are conserved in lymphotactin.

Vertebrate chemokine genes are closely clustered on discrete chromosomes according to their Cys-Cys or Cys-X-Cys family relation. For example, all previously reported Cys-Cys chemokines map to human chromosome 17 and mouse chromosome 11. Similarly, the Cys-X-Cys chemokines map to human chromosome four and, based on the similarities between mouse and human chromosomes, the Cys-X-Cys chemokines probably map to mouse chromosome five. Lymphotactin maps to the distal region of mouse chromosome one, which is linked to *Fasl*, *At3*, *Sele*, and *Otf1* (Fig. 2). Taken together with the sequence comparisons, these data support the hypothesis that lymphotactin represents the structural prototype of a new chemokine class.

Lymphotactin is abundant in the pro-T cell cDNA library; it is present at a frequency of 1 in 125 clones. Lymphotactin was also isolated from a cDNA library generated from $\alpha\beta TCR^+CD4^-CD8^-$ [αβ double negative (DN)] thymocytes (*8*). RNA blot analysis of T cell subsets confirmed that lymphotactin was present in activated, but not freshly isolated, pro-T cells (Fig. 3). A very high level of expression of lymphotactin was detected in both activated thymic $CD8^+CD3^+$ cells and activated $CD8^+CD3^+$ T cells derived from the spleen (Fig. 3). A very low level

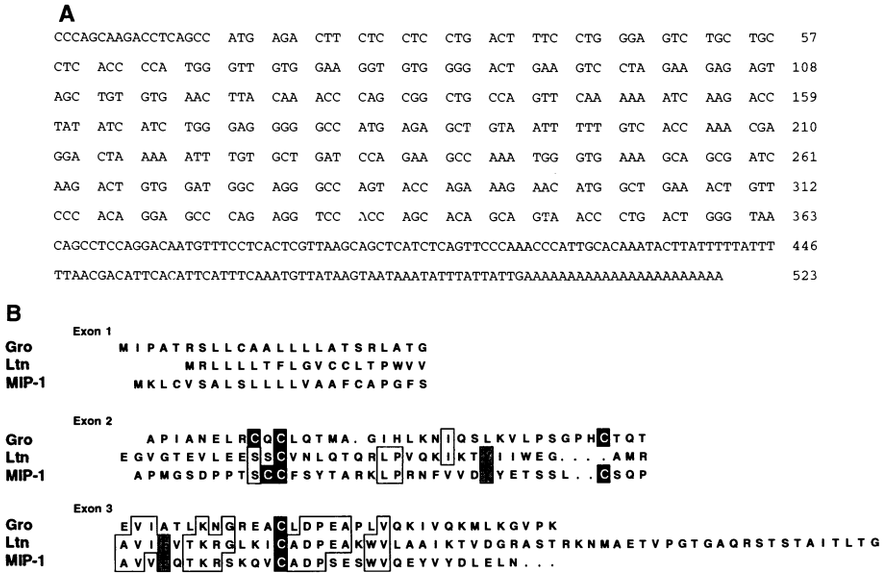

Fig. 1. The pro-T cell cDNA library was generated and screened (*19*, *20*). (**A**) The cDNA clones were sequenced with double-stranded templates and a sequence kit. Obtained sequences were compared to previously reported sequences in the data banks with FASTDB (Intelligenetics, Mountain View, California). (**B**) Lymphotactin (Ltn) amino acid sequence is aligned with the Cys-X-Cys chemokine Gro-α and the Cys-Cys chemokine MIP-1β (*21*). Exon organization represented is based on MIP-1β. Boxed residues are homologous between the two sequences. Black boxed residues represent the four cysteine residues that are diagnostic of both the Cys-X-Cys and Cys-Cys chemokine families. In addition, the shaded boxes represent the residues that are diagnostic of the Cys-Cys chemokine family (*7*).

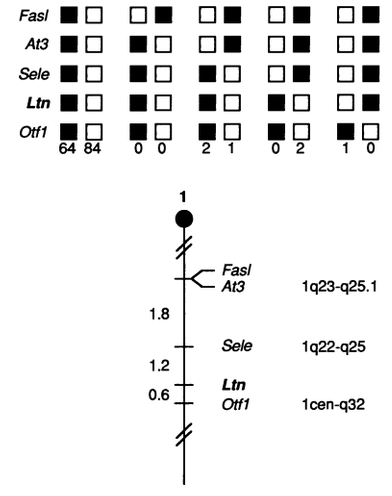

Fig. 2. *Ltn* maps in the distal region of mouse chromosome one. *Ltn* was placed on mouse chromosome one by interspecific backcross analysis (*22*). The segregation patterns of *Ltn* and flanking genes in 154 backcross animals that were typed for all loci are shown at the top of the figure. For individual pairs of loci, more than 154 animals were typed. Each column represents the chromosome identified in the backcross progeny that was inherited from the (C57BL/6J × *M. spretus*) F_1 parent. The black boxes represent the presence of a C57BL/6J allele, and white boxes represent the presence of an *M. spretus* allele. The number of offspring inheriting each type of chromosome is listed at the bottom of each column. A partial linkage map of chromosome one, showing the location of *Ltn* in relation to linked genes, is shown at the bottom of the figure. Recombination distances between loci are shown in centimorgans to the left of the chromosome, and the positions of loci in human chromosomes, where known, are shown to the right. Gene encoding lymphotactin is indicated by *Ltn*, gene encoding Fas ligand by *Fasl*, gene encoding antithrombin 3 by *At3*, gene encoding selectin endothelium by *Sele* (formerly *Elam*), and gene encoding octamer-binding transcription factor 1 by *Otf1*.

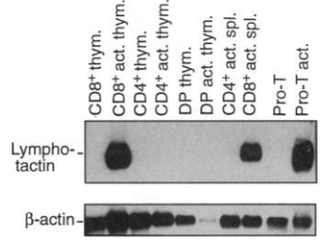

Fig. 3. RNA blot of lymphocyte subsets. Polyadenylated RNA was isolated from sorted cell populations from the thymus (thym.) and spleen (spl.) (*23*). The number of cells used to generate mRNA employed in the RNA blot was similar for all cell types and was confirmed by hybridization with β-actin. The weak β-actin signal detected on activated (act.) DP cells is most likely due to programmed cellular degradation known as apoptosis, which occurs when DP cells are activated.

of expression in activated mature $CD4^+$ thymocytes was detected. This weak hybridization signal may be due to the small subpopulation of $CD4^+$ $NK1.1^+$ cells that are present in total $CD4^+$ T cells (9). The $CD4^+$ $NK1.1^+$ T cells have characteristics similar to those of the αβ DN T cells that produce lymphotactin, in that both cell types are biased toward $V_\beta 8.2$ in their T cell receptor repertoire, both produce high titers of IL-4 without being T helper cell type 2 ($T_H 2$), and both are major histocompatability complex class I–restricted. There was no detectable expression of lymphotactin in activated $CD4^+CD8^+$ [double positive (DP)] thymocytes. Furthermore, hybridization to a mouse multiple tissue RNA blot failed to detect lymphotactin in heart, brain, spleen, lung, liver, kidney, testis, or skeletal muscle tissue.

Recombinant lymphotactin was generated by expression in *Escherichia coli* (*10*) and tested for biological activity. A defining characteristic of chemokines is their ability to induce a chemotactic response in cells of the immune system (*11*, *12*). A cell type will demonstrate chemotaxis to a relatively narrow concentration range of chemokine in vitro—too high a concentration causes adhesion, and too low a concentration will not elicit chemotaxis (*13*). In order to assess the chemotaxis induced by lymphotactin, several leukocyte populations were tested for their ability to migrate in response to lymphotactin. Qualitative interpretation of the meaning of the chemotactic response in comparing one cell population to another is determined by several characteristics: the absolute number of cells that demonstrate chemotaxis, the concentration of factor that elicits the maximum chemotactic response, and the difference in number of cells that migrate from the least to the most optimal concentration.

As seen in Fig. 4, a variety of cells demonstrate a dose-dependent chemotactic response to lymphotactin. Among the most responsive cells were $CD4^+$-depleted thymocytes, which are enriched for $CD8^+$ thymocytes (Fig. 4B), and DN thymocytes (Fig. 4J), in which a 10^{-10} M concentration induced chemotaxis. In contrast, a 10^{-8} M concentration was required to induce a chemotactic response in thymic $CD8^+$-depleted cells, which are enriched for $CD4^+$ T cells. This parallels the response of these two cell types to MIP-1α. The chemotactic responses of T cell–depleted spleen cells, day 15 fetal liver cells, bone marrow cells, and lymph node cells were comparable with the response of thymic $CD8^+$-depleted cells. These cell populations demonstrated a similar chemotactic response to MIP-1α. Unlike MIP-1α, lymphotactin did not induce a chemotactic response in either peritoneal exudate cells (Fig. 4H) or in the cells of human monocytic cell line THP-1 (Fig. 4I). Further analysis of monocyte-macrophage populations derived from a variety of sources as well as neutrophils supported the conclusion that lymphotactin does not induce chemotaxis in monocyte-macrophages or neutrophils. In addition, thymic $CD4^+$ $CD8^+$ cells did not demonstrate chemotaxis to lymphotactin.

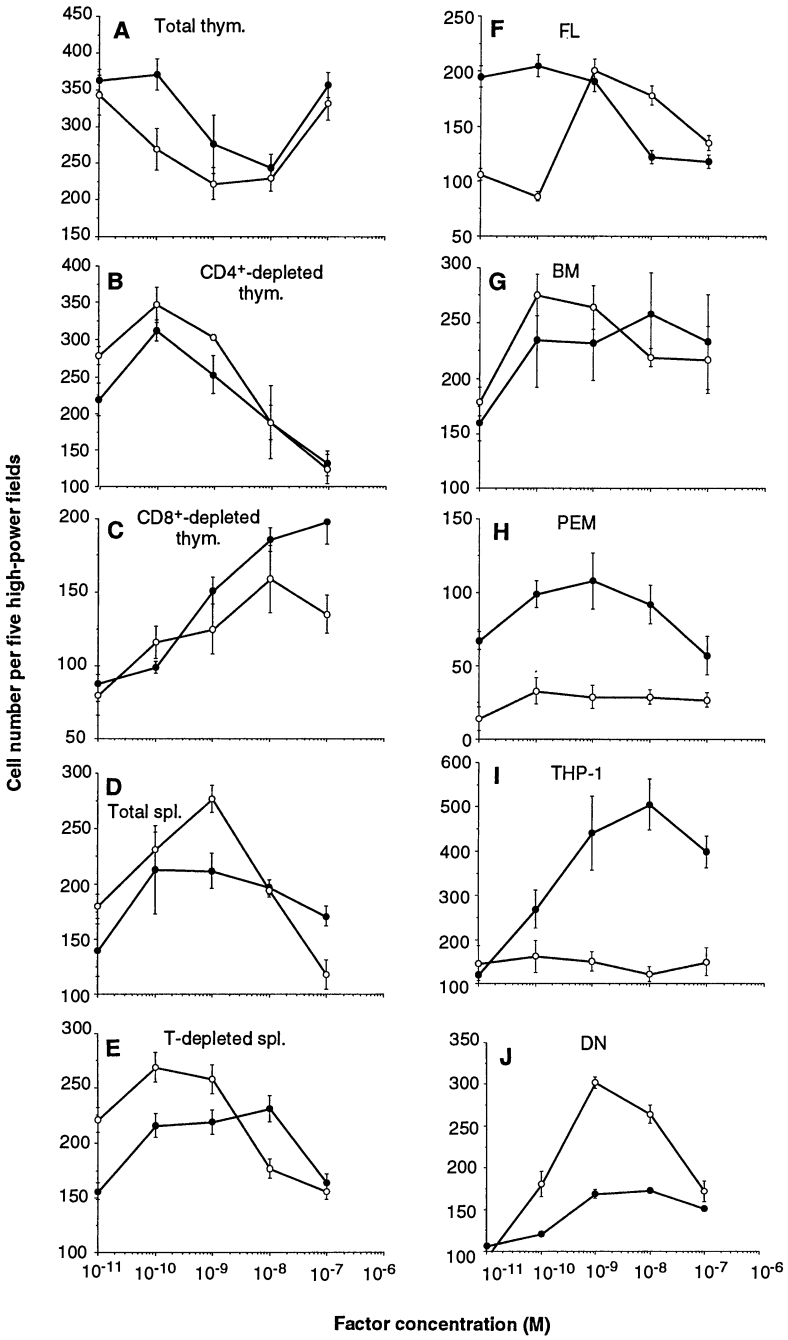

Fig. 4. Lymphocytes are chemotactic in response to lymphotactin. Chemotaxis assays were done with 48-well microchemotaxis apparatus as previously described (*24*). Migration is expressed as cell number per five high-power fields (×400), with duplicate wells being counted for each of three experiments. Closed circles represent MIP-1α; open circles represent lymphotactin. All cells were obtained from BALB/c mice unless otherwise noted. Number of cells in the negative control of media alone is indicated. (**A**) Total thymocytes (media = 128 ± 12). (**B**) $CD4^+$-depleted thymocytes (media = 112 ± 3). (**C**) $CD8^+$-depleted thymocytes (media = 70 ± 9). (**D**) Total spleen cells (media = 86 ± 4). (**E**) $CD4^+CD8^+$-depleted splenocytes (media = 80 ± 30). (**F**) Day 14 fetal liver cells (media = 128 ± 8). (**G**) Bone marrow cells (media = 112 ± 8). (**H**) Peritoneal exudate macrophages (media = 61 ± 17). (**I**) Cells from human monocytic cell line THP-1 (media = 157 ± 43). (**J**) $CD4^+CD8^+$-depleted thymocytes (media = 93 ± 7).

In order to distinguish between chemotaxis (directed movement) and chemokinesis (increased random movement), a modified filter-based assay system was used (*13*). $CD8^+$-depleted thymocytes, $CD4^+$-deplet-

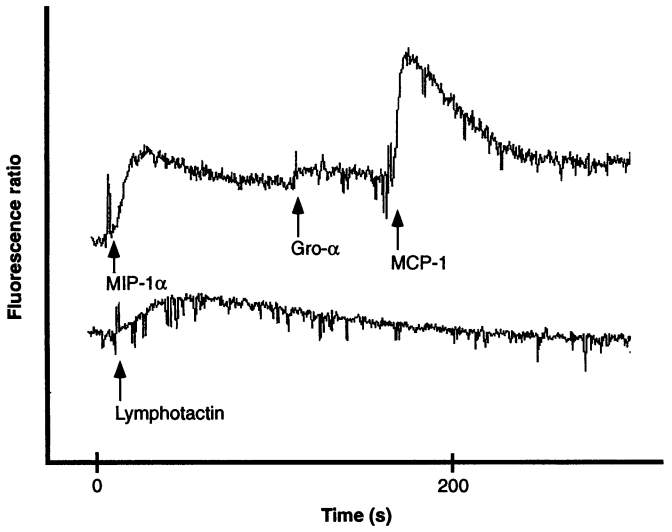

Fig. 5. Ca^{2+} flux on T cells. $CD4^+$-depleted thymocytes were loaded in the presence of 3 μM INDO 1/AM (Calbiochem). Fluorescence was measured on a PTI spectrofluorometer at an excitation wavelength of 350 nm. Dual simultaneous emissions were recorded at 400 and 490 nm. Ratios were calculated at two points per second. Fluorescence ratio equals 400:490 nm. Arrows indicate points where the factors were added to the cells [MIP-1α (10^{-6} M), Gro-α (10^{-6} M), lymphotactin (10^{-6} M), and MCP-1 (10^{-6} M)].

ed thymocytes, and DN thymocytes were assayed for chemokinesis. None of these cell populations demonstrated chemokinesis. This further supports the idea that lymphotactin is a chemotactic factor. Therefore, lymphotactin appears to be unique among chemokines in that it induces chemotactic responses only in lymphoid populations.

In general, when Cys-Cys chemokines bind their receptor on leukocytes there is a measurable intracellular Ca^{2+} flux (*14*). Therefore, we examined the ability of lymphotactin to initiate Ca^{2+} flux in $CD4^+$-depleted thymocytes, because these cells demonstrated a potent chemotactic response to lymphotactin. As seen in Fig. 5, lymphotactin was able to generate a small but significant Ca^{2+} flux in these cells. In addition, MIP-1α, Gro-α, and monocyte chemotactic protein 1 (MCP-1) were able to generate a Ca^{2+} flux in this population. This result suggests that a small subpopulation of the $CD4^+$-depleted thymocytes employ Ca^{2+} signaling in response to lymphotactin. Whether this is the same population of cells that respond chemotactically to lymphotactin is not known. Also, it is not known whether alternative signaling mechanisms that do not involve Ca^{2+} may be employed by these cells in response to lymphotactin.

Taken together, both the structural and biological data support the view that lymphotactin represents a new class of chemokine. The chemotactic studies suggest that lymphotactin is specific for lymphocytes. If this holds true, it will be the first example of a lymphocyte-specific chemokine. This chemokine is unlikely to represent an anomalous occurrence, because we have recently isolated a cDNA encoding human lymphotactin (*15*). The structure of the human gene encoding lymphotactin shares the unique characteristic of the mouse gene in regard to the cysteine residues. Based on this data, and on the chromosome mapping and the sequence data, we propose that lymphotactin does not belong to the Cys-Cys or Cys-X-Cys chemokine family. Instead, it may represent the first known member of a new class of chemokines that we propose be designated the C family of chemokines.

REFERENCES AND NOTES

1. D. I. Godfrey and A. Zlotnik, *Immunol. Today* **14**, 547 (1993).
2. D. I. Godfrey, J. Kennedy, P. Mombaerts, S. Tonegawa, A. Zlotnik, *J. Immunol.* **152**, 4783 (1994).
3. D. I. Godfrey, J. Kennedy, T. Suda, A. Zlotnik, *ibid.* **150**, 4244 (1993).
4. S. F. Altschul, W. Gish, W. Miller, E. W. Myers, D. J. Lipman, *J. Mol. Biol.* **215**, 403 (1990).
5. G. Davatelis *et al.*, *J. Exp. Med.* **167**, 1939 (1988).
6. P. J. Lodi *et al.*, *Science* **263**, 1762 (1994).
7. A. Bairoch, *Nucleic Acids Res.* **21**, 3097 (1993).
8. A. Zlotnik, D. I. Godfrey, M. Fischer, T. Suda, *J. Immunol.* **149**, 1211 (1992).
9. H. Arase, N. Arase, K. Ogasawara, R. A. Good, K. Onoe, *Proc. Natl. Acad. Sci. U.S.A.* **89**, 6506 (1992).
10. PCR was used to modify the lymphotactin cDNA in order to insert a Hind III restriction site proximal to Gly^2 (1 being the expected NH_2-terminal residue of the mature secreted protein) and an Xho I site distal to the translation stop codon of the open reading frame. The resulting Hind III–Xho I fragment was inserted into Hind III– and Xho I–cleaved pFLAG-1 plasmid (International Biotechnologies, New Haven, CT). The resulting expression plasmid was transformed into the Topp5 *E. coli* strain (Stratagene) and ampicillin-resistant (50 μg/ml) transformants were grown in Luria broth (Gibco) at 37°C until the optical density at 550 nm was 0.7. Recombinant protein was induced with 0.4 mM isopropyl β-D-thiogalactopyranoside (Sigma), and incubation of the cells continued at 20°C for a further 18 hours. Cells from a 1-liter culture were harvested by centrifugation and resuspended in 200 ml of ice-cold 30% sucrose, 50 mM tris-HCl (pH 8.0), and 1 mM ethylenediaminetetraacetic acid. After 10 min on ice, ice-cold water was added to a total volume of 2 liters. After 20 min on ice, cells were removed by centrifugation, and the supernatant was clarified by filtration with a 5 μM Millipak 60 (Millipore, Bedford, MA). The recombinant protein was purified with a 25-ml M2 affinity matrix (International Biotechnologies) after being cycled at 200 ml/hour for 48 hours at 4°C, washed with phosphate-buffered saline (PBS), eluted with 0.1 M glycine HCl (pH 3.0), and neutralized with tris-HCl to pH 8.0. The recombinant protein was buffer-exchanged in PBS.
11. T. J. Schall, *Cytokine* **3**, 165 (1991).
12. J. J. Oppenheim, C. O. Zachariae, N. Mukaida, K. Matsushima, *Annu. Rev. Immunol.* **9**, 617 (1991).
13. S. H. Zigmond and J. G. Hirsch, *J. Exp. Med.* **137**, 387 (1973).
14. K. Neote, G. D. Di, J. Y. Mak, R. Horuk, T. J. Schall, *Cell* **72**, 415 (1993).
15. J. Kennedy and A. Zlotnik, in preparation.
16. J. F. Elliott *et al.*, *Proc. Natl. Acad. Sci. U.S.A.* **87**, 6363 (1990).
17. N. G. Copeland and N. A. Jenkins, *Trends Genet.* **7**, 113 (1991).
18. N. A. Jenkins, N. G. Copeland, B. A. Taylor, B. K. Lee, *J. Virol.* **43**, 26 (1982).
19. Pro-T cells ($CD44^+25^+3^-4^-8^-$) from BALB/c mice were prepared for sorting on a fluorescence-activated cell sorter by being labeled with appropriate antibodies as previously described (*3*). Sorted pro-T cells were activated for 6 hours with calcium ionophore A23187 (Calbiochem) (resuspended to 1 mM dimethyl sulfoxide and used at a final concentration of 0.35 μM), PMA (Calbiochem) (resuspended to 1 mg/ml in ethanol and used at 10 ng/ml), and IL-1 (Genzyme, Cambridge, MA) (20 U/ml) and then cultured in IL-7, stem cell factor, and IL-2 for 9 to 12 days to allow them to expand. Cells were then reactivated for 6 hours before being harvested and stored at −70°C. In order to assess the quality of the second activation, an aliquot of cells was transferred to fresh complete media after the 6 hours of activation and cultured overnight. Supernatant from these cultures was assayed on the IL-2–dependent cell line HT-2. Only cultures that showed high titers of IL-2 after activation were used in generating the cDNA libraries. In this manner, cells were accumulated and later pooled to isolate mRNA. The D10.G4.1 T cell line, which demonstrates a T_H2 phenotype; the HC7 T cell line, which demonstrates a T_H1 phenotype; and the HT-2 T cell line, which was used as a "housekeeping gene" T cell line, were used to make cDNA libraries for screening the pro-T cell cDNA library. The D10.G4.1 line was expanded in culture and activated on culture plates coated with antibody to CD3 (Pharmingen) (10 μg/ml) for 6 hours before being harvested and stored at −70°C. These cells were assayed for quality of activation as described above. The HT-2 cells were expanded in culture media containing IL-2 (490 U/ml), washed in PBS, and stored at −70°C.
20. The mRNA was prepared with the FastTrack kit (Invitrogen), from which cDNA was generated by use of the SuperScript plasmid system for cDNA synthesis from Gibco-BRL (Gaithersburg, MD), essentially as described by the manufacturer. One modification to the procedure was the substitution of Bst XI adapters (Invitrogen) for the Sal I adapters provided with the kit. The resultant cDNA from these cells was used to generate libraries in the plasmid PCDNA II (Invitrogen). The cDNA was cloned into the Bst XI–Not I site in the polylinker and was used to transform the DH10B strain of *E. coli*. Plasmid was isolated and purified with the Qiagen system (Chatsworth, CA), which was used to generate RNA probes from the SP6 promoter. A second cDNA library from the pro-T cells was generated in the Bst XI–Not I polylinker of the plasmid pJFE14 SR alpha (*16*). This library was used to transform DH10B, and the bacteria were plated on agarose, transferred to nylon membranes in triplicate, and screened with RNA probes from the other libraries. The screening approach used was termed differential screening. In general, this procedure uses RNA probes generated from two categories of cDNA libraries. The first category contains probes from cDNA libraries generated from cell types that are not to be characterized. The cDNA libraries used in this screening were generated as described above from D10.G4.1, HC7, and HT-2 T cell lines in the PCDNA I or PCDNA II plasmid (Invitrogen) containing an SP6 and a T7 promoter. The second category contains probes from the cDNA library to be characterized. The cDNA library used in this screening was prepared from the

pro-T cells as described above. The RNA probes were labeled by means of the Genius system (Boehringer Mannheim), as described by the manufacturer. However, both the SP6 and T7 RNA polymerase used were obtained from Promega (Madison, WI). The HT-2 probe and pro-T cell probe were each used at 10 ng/ml, and the HC7 and D10.G4.1 probes were each used at 5 ng/ml and were combined into one probe mix. The filter lifts of the pro-T cell pJFE cDNA library were prehybridized at 42°C for 3 to 6 hours in Church's buffer [50% formamide, 6× saline–sodium phosphate–EDTA buffer, 50 mM $NaHPO_4$ (pH 7.2), 7% SDS, 0.1% *N*-lauryl sarcosine, and 2% Boehringer Mannheim blocking reagent]. Filters were probed overnight in the same buffer containing the appropriate probe. Specifically, each filter from the set of triplicate filters was probed with HT-2 RNA probes, pro-T cell RNA probes, or pooled HC7 + D10.G4.1 RNA probes. The filters were washed as described by the Genius system. Chemiluminescent detection of hybridization was used as described by the Genius system. The colonies that were positive for hybridization with the pro-T cell probe but not the HT-2 or D10.G4.1 + HC7 probes were selected as being potentially unique to the pro-T cell cDNA library. These clones were selected for sequencing.

21. Single-letter abbreviations for the amino acid residues are as follows: A, Ala; C, Cys; D, Asp; E, Glu; F, Phe; G, Gly; H, His; I, Ile; K, Lys; L, Leu; M, Met; N, Asn; P, Pro; Q, Gln; R, Arg; S, Ser; T, Thr; V, Val; W, Trp; and Y, Tyr.
22. Interspecific backcross progeny were generated by mating (C57BL/6J × *Mus spretus*) F_1 females and C57BL/6J males as described (*17*). A total of 205 N_2 mice were used to map the locus of the gene encoding lymphotactin, *Ltn*. DNA isolation, restriction enzyme digestion, agarose gel electrophoresis, Southern blot transfer, and hybridization were done essentially as described (*18*). All blots were prepared with Hybond-N nylon membrane (Amersham). The probe, an ~536–base pair fragment of mouse cDNA, was labeled with [^{32}P]deoxycytidine triphosphate (dCTP); washing was done to a final stringency of 0.1× sodium chloride, sodium citrate, and sodium phosphate and 0.1% SDS at 65°C. A fragment of 13.0 kb was detected in Sph I–digested C57BL/6J DNA, and a fragment of 8.6 kb was detected in Sph I–digested *M. spretus* DNA. The presence or absence of the 8.6-kb *M. spretus*–specific Sph I fragment was followed in backcross mice. Recombination distances were calculated with the computer program SPRETUS MADNESS (National Cancer Institute–Frederick, Research and Development, Frederick, MD). Gene order was determined by minimization of the number of recombination events required to explain the allele distribution patterns. The most likely gene order and the ratios of the total number of mice exhibiting recombinant chromosomes to the total number of mice analyzed for each pair of loci are: centromere—*Fasl*—0:180—*At3*—3:164—*Sele*—2:162—*Ltn*—1:170—*Otf1*. The recombination frequencies (expressed as genetic distances in centimorgans ± SEM) are: (*Fasl*, *At3*)—1.8 ± 1.1—*Sele*—1.2 ± 0.9—*Ltn*—0.6 ± 0.6—*Otf1*. References for the human map positions of loci cited in this study can be obtained from the Genome Data Base, a computerized database of human linkage information maintained by the William H. Welch Medical Library of The Johns Hopkins University (Baltimore, MD).
23. Polyadenylated RNA was isolated from sorted cell populations with the FastTrack mRNA kit (Invitrogen). Samples were electrophoresed in a 1% agarose gel containing formaldehyde and transferred to a GeneScreen membrane (NEN Research Products, Boston, MA). Hybridization was done at 65°C in 0.5 M $NaHPO_4$ (pH 7.2), 7% SDS, 1 mM EDTA, and 1% bovine serum albumin (fraction V) with [^{32}P]dCTP-labeled lymphotactin cDNA at 10^7 cpm/ml. After hybridization, filters were washed three times at 50°C in 0.2× standard saline citrate and 0.1% SDS and exposed to film for 24 hours.
24. K. B. Bacon, R. D. Camp, F. M. Cunningham, P. M. Woollard, *Br. J. Pharmacol.* **95**, 966 (1988).
25. We thank G. Zurawski for help in expressing recombinant lymphotactin and B. Behrens and D. J. Gilbert for excellent technical assistance. The GenBank accession number for the nucleotide sequence of lymphotactin is mLtn: U15607.

29 June 1994; accepted 6 September 1994

Long-Term Behavioral Recovery in Parkinsonian Rats by an HSV Vector Expressing Tyrosine Hydroxylase

Matthew J. During,* Janice R. Naegele, Karen L. O'Malley, Alfred I. Geller

One therapeutic approach to treating Parkinson's disease is to convert endogenous striatal cells into levo-3,4-dihydroxyphenylalanine (L-dopa)–producing cells. A defective herpes simplex virus type 1 vector expressing human tyrosine hydroxylase was delivered into the partially denervated striatum of 6-hydroxydopamine–lesioned rats, used as a model of Parkinson's disease. Efficient behavioral and biochemical recovery was maintained for 1 year after gene transfer. Biochemical recovery included increases in both striatal tyrosine hydroxylase enzyme activity and in extracellular dopamine concentrations. Persistence of human tyrosine hydroxylase was revealed by expression of RNA and immunoreactivity.

Parkinson's disease (PD), a neurodegenerative disorder, is characterized by the progressive loss of the dopaminergic neurons in the substantia nigra pars compacta that project to the corpus striatum (*1*). The principal therapy for PD is the oral administration of L-dopa (*2*), which is converted to dopamine (DA) by endogenous striatal aromatic amino acid decarboxylase (AADC) (*3*). Although it is initially effective, L-dopa therapy loses efficacy over a period of several years (*1*). Transplantation of cells that produce L-dopa or DA into the striatum can correct animal models of PD (*4*) but has not been a viable therapy in most human trials (*5*). Peripheral cell types that are genetically modified to express tyrosine hydroxylase (TH) and produce L-dopa have supported only short-term improvement (less than 2 months) in animal models of PD (*6*, *7*). Genetically modified muscle cells support longer improvements (6 months) (*8*), but the viability of a muscle cell graft in the human striatum is not yet clear. An alternative therapeutic strategy is to convert a fraction of the striatal cells into L-dopa–producing cells by expression of TH in striatal cells (*9*) from a defective herpes simplex virus type 1 (HSV-1) vector (*10*). Potential advantages of this approach include production of L-dopa at the required site of action, so that diffusion over substantial distances is not necessary, and alleviation of potential problems caused by graft rejection or tumor formation. To test this strategy, a human TH complementary DNA (cDNA) (form II) (*11*, *12*) was inserted into an HSV-1 vector (pHSVth). Infection of cultured striatal cells with pHSVth resulted in expression of human TH RNA, TH immunoreactivity, and the release of L-dopa into the culture medium (*13*). The amounts of L-dopa released per infected cell suggested that pHSVth might be evaluated in the 6-hydroxydopamine (6-OHDA)–lesioned rat, a model of PD.

pHSVth virus or pHSVlac virus or vehicle alone [phosphate-buffered saline (PBS)], was delivered by stereotactic injection into the partially denervated striatum of unilaterally 6-OHDA–lesioned rats (*14*). The apomorphine-induced rotation rate was measured as an index of behavioral recovery. The average decrease in the rotation rate caused by pHSVth was 64 ± 6% at 2 weeks after gene transfer. This value remained relatively constant over a 1-year period, and the decrease remained statistically significant at both 6 months ($P < 0.01$) and 1 year ($P < 0.05$) after gene transfer as compared with the control groups (Fig. 1A and Table 1). The rotation rate of each rat in the pHSVth group remained relatively constant and was similar to the rotation rate in the final test (Table 1).

TH enzyme activity and extracellular DA concentrations in the injected striatum were evaluated in selected rats 4 to 6

M. J. During, Departments of Surgery and Medicine, Yale University School of Medicine, New Haven, CT 06510, USA.
J. R. Naegele, Department of Biology, Wesleyan University, Middletown, CT 06457, USA.
K. L. O'Malley, Department of Anatomy and Neurobiology, Washington University School of Medicine, St. Louis, MO 63110, USA.
A. I. Geller, Division of Endocrinology, Children's Hospital, and Program in Neuroscience, Harvard Medical School, Boston, MA 02115, USA.
*To whom correspondence should be addressed.